Electron Microscopy of Transformation Induces Lattice Distortions in $TiHfZrNb_{0.3}$ Refractory High Entropy Alloys

Kaijun Yin[1,2], Xuesong Fan[3], Lia Amalia[3], Peter K. Liaw[3], and Jian-Min Zuo[1,2]

[1.] Department of Materials Science and Engineering,
[2.] Materials Research Laboratory, University of Illinois at Urbana-Champaign, Urbana, Illinois, 61801, United States of America
[3.] Department of Materials Science and Engineering, The University of Tennessee Knoxville, Knoxville, TN 37996, United States

Refractory high entropy alloys (RHEAs) are a subset of high entropy alloys (HEAs) composed primarily of refractory metals such as niobium, molybdenum, tantalum, titanium, hafnium [1, 2]. These alloys have attracted considerable interest for their remarkable ability to maintain strength at high temperatures [3]. However, only a few RHEA compositions are known to exhibit significant strain resistance exceeding 10% at room temperature [4, 5]. $TiHfZrNb_x$ is one example. With Nb in non-equimolar proportions, this alloy can improve the ductility with the hexagonal close-packed (HCP) phase transformation-induced plasticity (TRIP) [6, 7, 8]. This alloy also has a high density of fine ω particles that are often observed in conventional Ti alloys. However, the role of hexagonal ω phase in ductility is not clear.

In this study, two $TiZrHfNb_{0.3}$ samples were examined using advanced electron microscopy, including four-dimensional scanning transmission electron microscopy (4D-STEM) [Shao, Haw-Wen]. One of the samples is an as-cast alloy, which exhibits both high strength and great ductility, and the other is annealed at 1000°C for 6 hours and brittle. Microstructural analysis revealed a predominant body-centered cubic (BCC) phase in both specimens, with minor peaks indicative of the formation of ω phase in neutron diffraction. Electron diffraction patterns recorded from the two samples using 4D-STEM reveal the characteristic diffraction spots belonging to the ω phase between the brighter principal spots of the BCC structure (Figs. 1a, d). The distribution of the ω phase is mapped using the 4D-STEM datasets. The diffraction patterns are first transformed into difference cepstra using the method described by Shao et al. [ref]. The harmonic peaks belonging to the ω phase are identified and used to form images. These images show the distribution of nano-scaled ω phases within the BCC matrix (Figs. 1e, f). In the annealed sample, we observed the aggregation of ω phases compared to the random distribution in the as-cast sample.

Atomic-resolution analysis of the ω phase were carried out using an aberration corrected STEM and a high-angle annular detector for Z-contrast. These images shown in Fig. 2 reveal regions of the ω phase formation embedded in the BCC matrix. Within the BCC matrix, the atoms are also distorted. Fourier analysis of these regions also show the diffuse-like signals belonging to the ω phase. These diffuse features can be attributed to the transformation induced lattice distortion. The heat treatment reduces the sizes of the observed ω phase (Fig. 2). The change in the ω phase phase size and distribution can be correlated with the tensile experiments, which were conducted on the as-cast and heat-treated samples, which demonstrate the ductile to brittle transition.

Together, the above results demonstrate the critical role of the ω phase in the ductile to brittle transition in the RHEAs, the challenges, and opportunities for electron microscopy characterization, especially by combining 4D-STEM and atomic resolution imaging-based lattice distortion analysis.

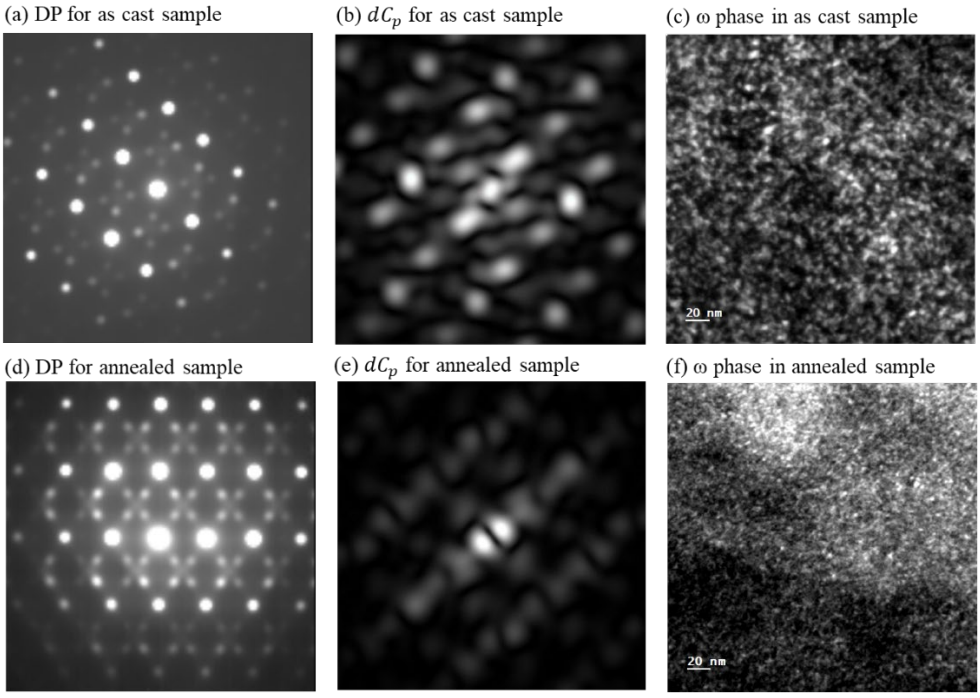

Fig. 1. (a,d) Averaged 4D-STEM diffraction pattern from as-cast and annealed sample along [110] zone, respectively. (b,e) Averaged difference Cepstral (dC_p) transformed electron nano-diffraction pattern. (c, f) C-STEM images used the ω phases signal in (b, e) to show the distribution of ω phase within the BCC matrix from two samples.

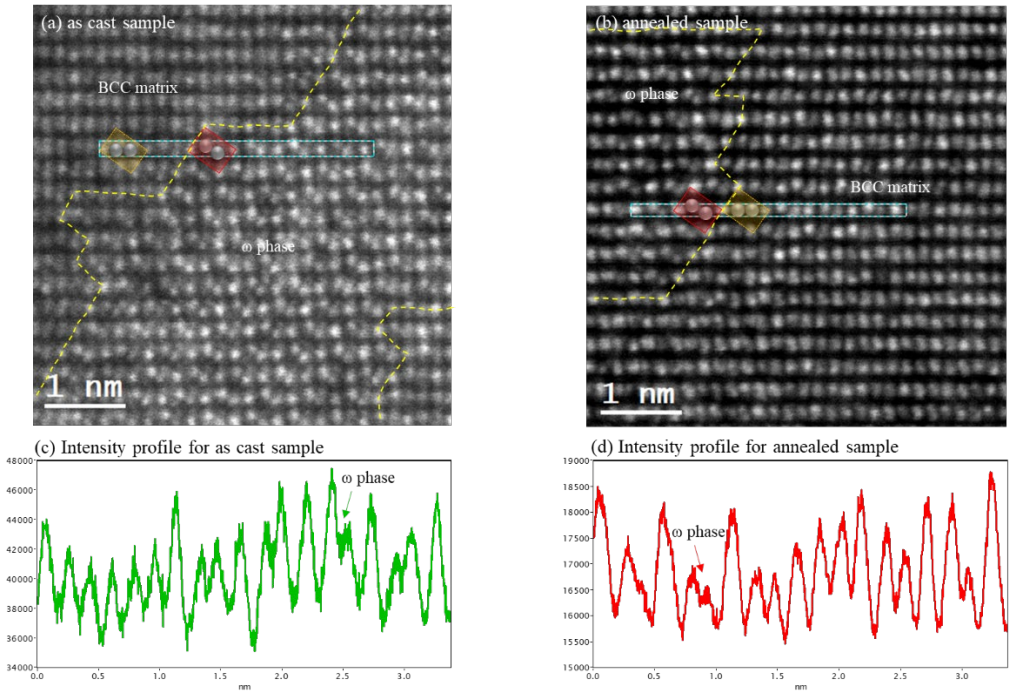

Fig. 2. Atomic resolution HAADF STEM images to show the atomic arrangement of the interface between the ω phase (red box) and BCC matrix (orange box) on $Nb_{0.3}$ samples under different treatment.

References

[1] O. N. Senkov, D. B. Miracle, K. J. Chaput, and J.-P. Couzinie, "Development and exploration of refractory high entropy alloys—A review," *Journal of Materials Research*, vol. 33, no. 19, pp. 3092–3128, Oct. 2018, doi: 10.1557/jmr.2018.153.
[2] O. N. Senkov, G. B. Wilks, D. B. Miracle, C. P. Chuang, and P. K. Liaw, "Refractory high-entropy alloys," *Intermetallics*, vol. 18, no. 9, pp. 1758–1765, Sep. 2010, doi: 10.1016/j.intermet.2010.05.014.
[3] C. Lee *et al.*, "Lattice distortion in a strong and ductile refractory high-entropy alloy," *Acta Materialia*, vol. 160, pp. 158–172, Nov. 2018, doi: 10.1016/j.actamat.2018.08.053.
[4] A. Detor, S. Oppenheimer, R. Casey, and C. Crawford, "Refractory high entropy alloy dataset with room temperature ductility screening," *Data in Brief*, vol. 45, p. 108582, Dec. 2022, doi: 10.1016/j.dib.2022.108582.
[5] Z. Li, K. G. Pradeep, Y. Deng, D. Raabe, and C. C. Tasan, "Metastable high-entropy dual-phase alloys overcome the strength–ductility trade-off," *Nature*, vol. 534, no. 7606, Art. no. 7606, Jun. 2016, doi: 10.1038/nature17981.
[6] L. Lilensten *et al.*, "Design and tensile properties of a bcc Ti-rich high-entropy alloy with transformation-induced plasticity," *Materials Research Letters*, vol. 5, no. 2, pp. 110–116, Mar. 2017, doi: 10.1080/21663831.2016.1221861.
[7] H. Huang *et al.*, "Phase-Transformation Ductilization of Brittle High-Entropy Alloys via Metastability Engineering," *Advanced Materials*, vol. 29, no. 30, p. 1701678, 2017, doi: 10.1002/adma.201701678.
[8] L. Zhang *et al.*, "Phase transformations in body-centered cubic NbxHfZrTi high-entropy alloys," *Materials Characterization*, vol. 142, pp. 443–448, Aug. 2018, doi: 10.1016/j.matchar.2018.06.012.
[9] Work supported by NSF, the Metals and Metallic Nanostructures Program (MMN) within the Division of Materials Research (DMR-2226495).